INTERFACE

rsif.royalsocietypublishing.org

Research

Cite this article: Zhang C, Adler PH, Monaenkova D, Andrukh T, Pometto S, Beard CE, Kornev KG. 2018 Self-assembly of the butterfly proboscis: the role of capillary forces. *J. R. Soc. Interface* **15**: 20180229.
http://dx.doi.org/10.1098/rsif.2018.0229

Received: 6 April 2018
Accepted: 4 July 2018

Subject Category:
Life Sciences–Physics interface

Subject Areas:
biomechanics, biophysics, bioengineering

Keywords:
butterfly proboscis, self-assembly, capillary force

Author for correspondence:
Konstantin G. Kornev
e-mail: kkornev@clemson.edu

Electronic supplementary material is available online at http://dx.doi.org/10.6084/m9.figshare.c.4162859.

THE ROYAL SOCIETY PUBLISHING

Self-assembly of the butterfly proboscis: the role of capillary forces

Chengqi Zhang[1], Peter H. Adler[2], Daria Monaenkova[1], Taras Andrukh[1], Suellen Pometto[2], Charles E. Beard[2] and Konstantin G. Kornev[1]

[1]Department of Materials Science and Engineering, and [2]Department of Plant and Environmental Sciences, Clemson University, Clemson, SC 29634, USA

KGK, 0000-0002-4513-1915

The proboscis of butterflies and moths consists of two C-shaped fibres, the galeae, which are united after the insect emerges from the pupa. We observed that proboscis self-assembly is facilitated by discharge of saliva. In contrast with vertebrate saliva, butterfly saliva is not slimy and is an almost inviscid, water-like fluid. Butterfly saliva, therefore, cannot offer any viscoelastic adhesiveness. We hypothesized that capillary forces are responsible for helping butterflies and moths pull and hold their galeae together while uniting them mechanically. Theoretical analysis supported by X-ray micro-computed tomography on columnar liquid bridges suggests that both concave and convex liquid bridges are able to pull the galeae together. Theoretical and experimental analyses of capillary forces acting on natural and artificial proboscises show that these forces are sufficiently high to hold the galeae together.

1. Introduction

The feeding device (proboscis) of butterflies and moths consists of a pair of C-shaped fibres, the maxillary galeae [1]. The two galeae form separately during the pupal stage and typically are assembled by a defined sequence of repeated actions into the united proboscis when the insect emerges from the pupa [2–4] (figure 1*a*). Each galea is a functional unit equipped with internal muscles, nerves, tracheae and blood (figure 1*b*) [1,5]. When the two galeae are united, the proboscis becomes a tube-like device, and the C-halves form a food canal (figure 1*b*) through which liquid is delivered to the gut, aided by a suction pump in the head [6–8].

The galeae of the long-tongued moths and butterflies are joined by a series of cuticular projections called legulae (figure 1*b*); the galeal musculature of these lepidopterans is fully developed to allow each galea to perform complex manoeuvres [1,3,9]. The two galeae, united as the proboscis, function as a single organ during routine use by the insect.

We hypothesize that butterflies rely on natural physical phenomena acting independently and without muscle actuation to help unite the galeae into the proboscis. A theoretical investigation of biomechanical causes of galeal attraction becomes important for understanding assembly of the lepidopteran proboscis.

An important clue in developing our hypothesis was previously suggested by biologists when they noticed that assembly of the proboscis is accompanied by the appearance of saliva [1–3,6] (figure 1*c*). Previous workers [1] have suggested that saliva acts as an adhesive gluing the galeae together. The gluing action of a liquid assumes its sliminess and stickiness. The saliva of butterflies has no mucin or other proteins imparting sliminess or viscoelasticity to the fluid, but instead follows purely Newtonian behaviour and is nearly inviscid [10]. Therefore, while appreciating the important role of saliva during proboscis assembly, we hypothesize that Lepidoptera rely on capillary action of salivary bridges to pull and hold the galeae together while the insect

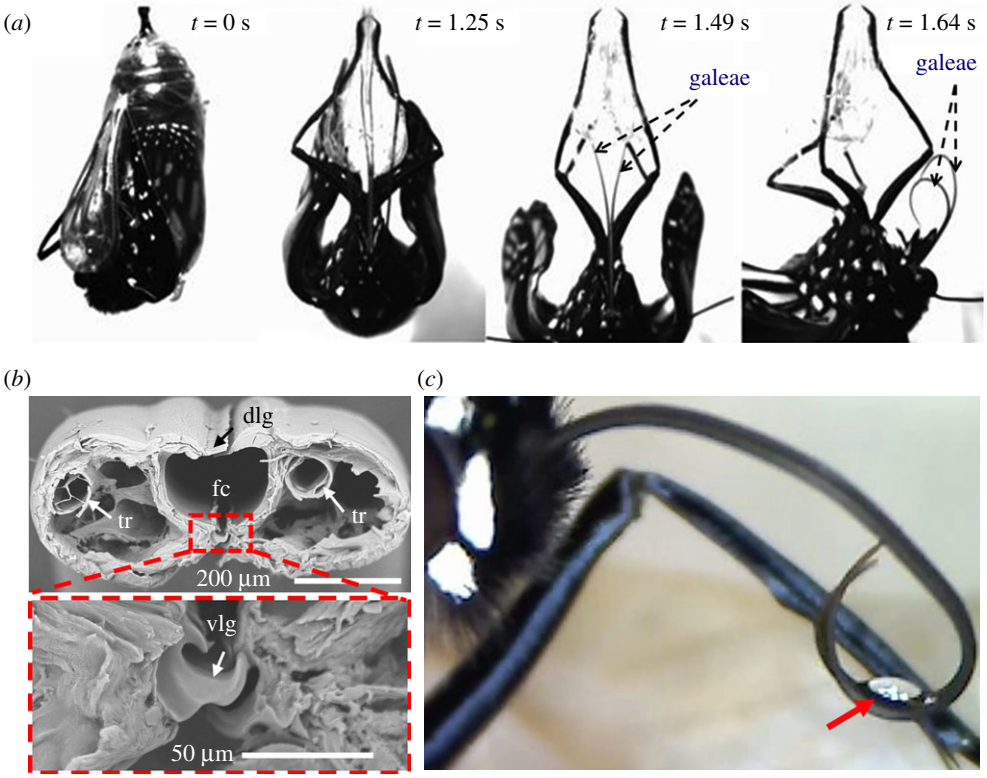

Figure 1. Monarch butterfly (*D. plexippus*). (*a*) Adult emerging from the pupa. The galeae of the proboscis are initially two separate strands. Emergence of the insect and proboscis assembly were tracked at 100 fps, using a Sony Pro Camera DSLR A100. (*b*) Cross section of the proboscis; each galea contains a trachea (tr), muscles and blood enclosed by a cuticular wall. When the galeae are united, at the dorsal legulae (dlg) and ventral legulae (vlg), their C-shaped walls form the food canal (fc). Magnification of the boxed area reveals the linkage mechanism formed by the legulae at the ventral side of the proboscis. (*c*) Drops of saliva are typically observed during proboscis assembly. A saliva droplet (arrow) is visible on the ventral side of the proboscis between the two galeae, which are not yet united.

mechanically couples the two strands. The most familiar expression of this capillary effect is the coalescence of wet hair [11].

To evaluate our hypothesis of capillary-assisted gathering of the galeae, we provide an analysis of the action of a saliva column spreading along the length of the food canal including along the half of each separated galea. The distribution of saliva over the length of the separated galeae was specified using micro-computed tomography (micro-CT). With specified meniscus configurations, we set up a model for an intergaleal saliva column and theoretically found the critical conditions when this column can hold the galeae together. We then used our model to estimate the capillary forces acting on the galeae and tested its predictions on artificial plastic proboscises. We concluded that the forces are strong enough to hold the galeae in proximity to each other while the insect couples the legulae.

2. Behavioural features of proboscis assembly

2.1. Structural features of the lepidopteran proboscis

The two galeae are coupled by ventral and dorsal arrays of legulae (figure 1*b*) that are differently shaped [6,9]. Ventral legulae consist of adjacent hooks that hold the galeae together yet allow longitudinal sliding (figure 1*b*). The dorsal legulae typically do not couple, but instead overlap or abut. The legulae and food canal are hydrophilic; for example, a water meniscus forms an approximately 45° contact angle with the food canal wall of the proboscis of the monarch butterfly (*Danaus plexippus*) [7,12].

2.2. Role of saliva in proboscis assembly

When the galeae are separated, we noticed that the butterfly produces saliva during the assembly (figure 2). However, saliva does not continuously wick into the gap separating the galeae. The release and retraction of saliva are controlled by a muscular pump in the butterfly's head, as inferred from our observations and those of Krenn [3]; saliva droplets periodically appear and disappear, suggesting that the insect produces saliva droplets as needed. Once released, saliva moves to the internal surface of the coil and collects at the point where the galeae are separated. This drop bridges the separated galeae. The butterfly pushes the drop back and forth and coils and uncoils the proboscis, adjusting the coil radius to ensure that the drop is placed in a position to hold the branching galeae together. We have previously discussed the physical mechanisms of drop formation on the inner margin of the coiled proboscis [13].

Proboscis assembly involves repetitive coiling and uncoiling and sliding of the galeae over one another in antiparallel movements, accompanied by discharge of saliva between the galeae. Coiling and uncoiling help align the separated galeae when they are sometimes slightly entangled with one another [3]. Antiparallel movements putatively contribute to galeal coupling of the ventral legulae [14]. Joining the galeae proceeds from the base to the apex of the proboscis and is facilitated by saliva [8]. Coiling and uncoiling the proboscis by the butterfly does not change the assembly scenario: the butterfly continues releasing saliva that bridges the galeae together until they are united [15].

During proboscis assembly, we observed saliva spreading over the medial surface of the galeae, forming a liquid

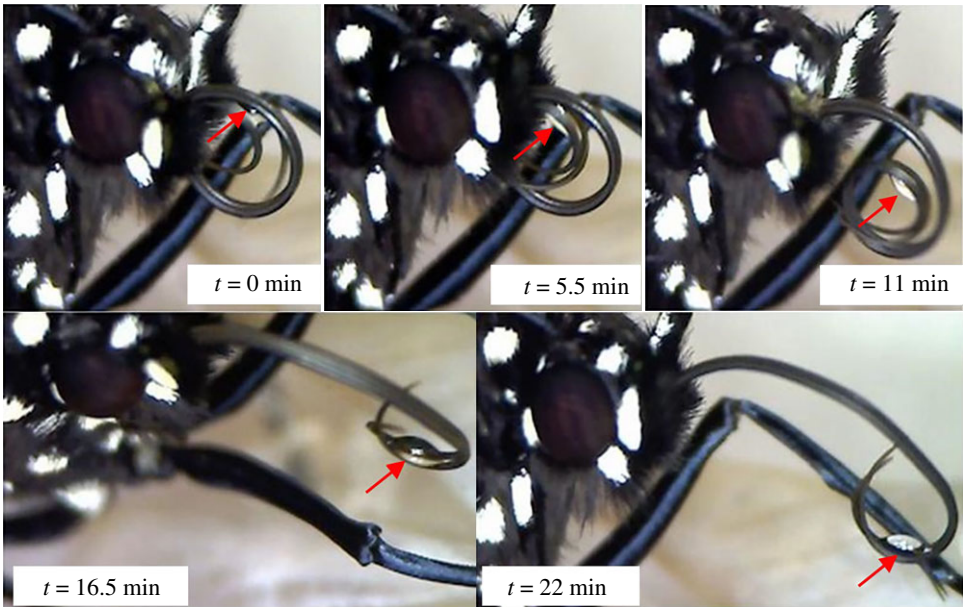

Figure 2. Saliva droplets are seen between two separated galeal strands of a just-emerged monarch butterfly ($t = 0$ min). When the proboscis is coiled, the drop is released near the head ($t = 5.5$ min). The drop of saliva then appears where the galeae are separated ($t = 11$ min). The proboscis is uncoiled ($t = 16.5$ and 22 min) and the galeae are brought together by the capillary effect. Drop release was tracked at 30 fps, using a digital microscope (GSI® GWC60-1).

column with menisci facing the air from the anterior and posterior ends of the proboscis (figures 2 and 3). The surface tension of the air–saliva interface, together with capillary pressure under the menisci, would force the two galeae together. Our observations suggested that saliva can propagate along the entire length of the separated galeae while the butterfly is uniting them. However, optical imaging does not allow these observations to be validated, and the opportunity to capture proboscis self-assembly in the brief period (within approx. 1 h) following emergence limits experimental investigation. We, therefore, used micro-CT on freshly killed insects to acquire the three-dimensional (3D) configuration of liquid menisci by scanning with X-ray imaging based on the density contrast of materials.

2.3. Menisci in completely separated galeae

A Bruker SKYSCAN 1176 Micro CT instrument was used in our experiments. It allows features of the meniscus/substrate pair to be identified with an accuracy of 9 µm. Therefore, the larger the proboscis, the better the resolution of the menisci. To increase the scale of the proboscis, we used the hawk moth *Manduca sexta*, which has a proboscis length of about 7 cm and food canal diameter (at mid-length) of about 80 µm. Hawk moths ($n = 5$) within 24 h after emergence from the pupa were frozen at −18°C overnight, allowing us to exclude the influence of insect motion while retaining a flexible (and assembled) proboscis. The proboscis was uncoiled, and the galeae were separated from the tip towards the head at an angle of about 20°, while ensuring that a section of the probosics near the head remained together. The separated tips of the proboscis were fixed to a plastic foam stage with double-sided tape to maintain the shape of the separated proboscis. The head of the moth, with the holder, then was attached to a half-cylindrical polystyrene foam stage designed to fit the micro-CT channel.

About 1 µl of OMNIPAQUE™ (iohexol) was injected at the vertex of the V-split galeae. It wetted the food canal and spread along the galeae. This liquid provides good contrast of menisci against other materials under the X-ray beam. Within 5 min after the contrast agent was fully spread and the menisci reached their equilibrium configurations, the sample was placed on the stage of the micro-CT instrument and scanned at 9 µm resolution. Five moths were used for the scan. Figure 3*c* shows an example of the cross-sectional shapes of the liquid body taken at different positions along the united part of the proboscis and separated galeae.

Hereafter, we refer to the liquid body in the region 'b'–'c' as the columnar bridge or liquid column. The liquid body in the region 'c'–'d' of the separated galea is the liquid finger, and the air–liquid interface in each cross section of the liquid body is the meniscus.

Three distinguishable configurations of meniscus profiles were observed. In the region where a segment of proboscis remained unseparated (position 'a' in figure 3*c*), the liquid formed a circular cylindrical column in the food canal of the united proboscis. Where the proboscis was separated at the vertex of the V (positions 'b' and 'c' in figure 3*c*), we observed a liquid bridge with two concave menisci indented towards the liquid interior; this liquid bridge connected the two separated galeae. We identified the shape of the liquid bridge as being formed by the two side arcs of the wall of the food canal and the two middle arcs as the interfaces of liquid and air.

In the region where the proboscis was fully separated (positions 'd' and 'e' in figure 3*c*), no liquid bridge was found; instead, we observed two separated liquid fingers running along the C-shaped walls of the galeae. The cross sections at different positions in this region show that the fingers formed a crescent moon-shaped cross section in each half of the food canal. The measured cross-sectional areas of the fingers along each semicircular half of the food canal remained almost the same (figure 3*d*), indicating each finger is a uniform liquid column. The average cross-sectional area of the liquid finger varies from one galea to the other, probably as a result of slight differences in the radius of the food canal and the wetting properties. The representative

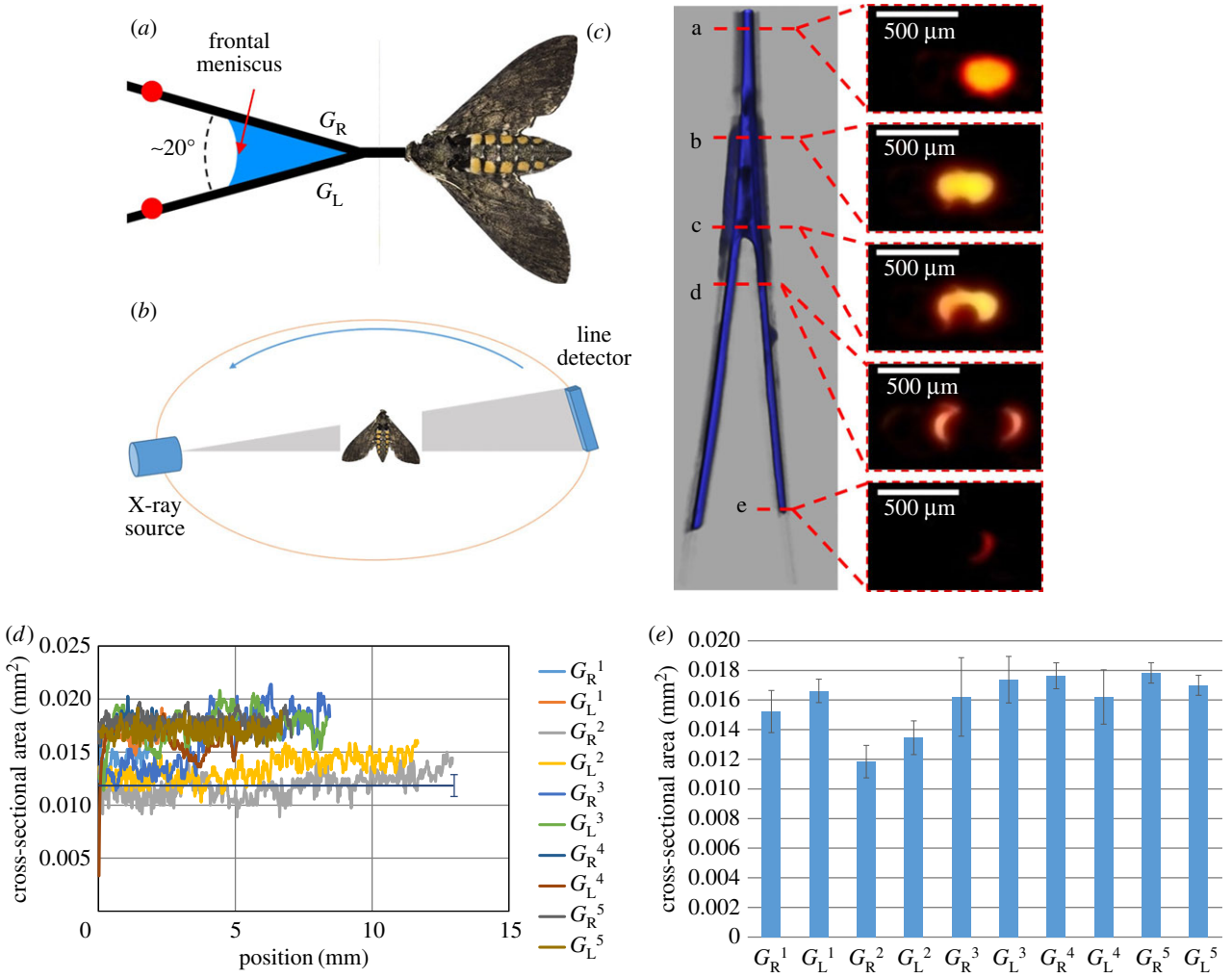

Figure 3. Modelling saliva action. (*a*) A hawk moth was pinned to the substrate, and the galeae were separated and straightened. Two pins (red dots) held the two galeae (subscripts 'R' (G_R) and 'L' (G_L) identify the right and left galae (G) as seen from the dorsal side of the proboscis) at the tips. A contrast agent, OMNIPAQUE™ (iohexol), was injected at the vertex of the V-split galeae. A liquid bridge (blue curved triangle) was observed. (*b*) In the Bruker SKYSCAN 1176 instrument, the moth was stationary while the X-ray source and detector acquired images. (*c*) An illustrative example of the cross-sectional shapes of the liquid column taken at different positions along the proboscis from (e) to (a). The liquid finger with almost constant radius of curvature spreads over the 'd'–'e' span and ends at position 'e'. The frontal meniscus at 'c' has a complex saddle-like shape. The columnar liquid bridge spreads over the 'b'–'c' span. (*d*) Cross-sectional area of the liquid finger versus position along the separated galeae for different individuals; the zero point is taken at the galeal tip. The grey dataset for galea G_L^2 (i.e. the left galea of the second individual) is shown as a straight line (the mean) and its error bar (standard deviation). (*e*) Summary for the cross-sectional area of a liquid finger situated in each separated galea of five different individual moths; the solid blue bar represents the mean of all micro-CT measurements along each galea, and the error bar represents the standard deviation of these measurements.

images for the measurements of the cross-sectional area of the liquid finger for each individual are in the electronic supplementary material, figure S6.

These observations suggest that the surface properties and geometrical shapes of the C faces of the galeae do not typically differ from one individual to another. The constancy of the finger cross-sectional areas over a long period of time (greater than 20 min) of micro-CT scanning suggests that the liquid fingers coexist in equilibrium with the liquid bridge. Accordingly, the formed fingers can be used for characterization of the wetting properties of the food canal.

Our experiment with live hawk moths and our observations of proboscis self-assembly of live monarch butterflies and painted lady butterflies (*Vanessa cardui*) assembling their proboscises allow us to conclude that (i) saliva forms a cylindrical column in the unseparated food canal and (ii) a liquid bridge forms at the conjunction of galeal separation. Experiments on freshly dead insects show that two liquid fingers form with crescent moon-shaped cross sections in the semicircular walls of the food canal of each galea. Based on this imaging, we built the model of a liquid bridge connecting the separated galeae.

3. Model formulation

According to our observations, the galeae come together only when their edges are aligned almost parallel to one another. Saliva is always present during proboscis self-assembly and is pumped by the insect until the galeae unite. Therefore, the saliva column bridging the galeae together seems to facilitate galeal assembly.

Our observations on live butterflies and those of Krenn [3] revealed that, in the vicinity of the point where the galeae begin to separate, the radius of curvature of the proboscis coil is always much larger than the intergaleal distance. Therefore, when evaluating the capillary force acting on the galeae, as a first approximation, we can consider the galeae

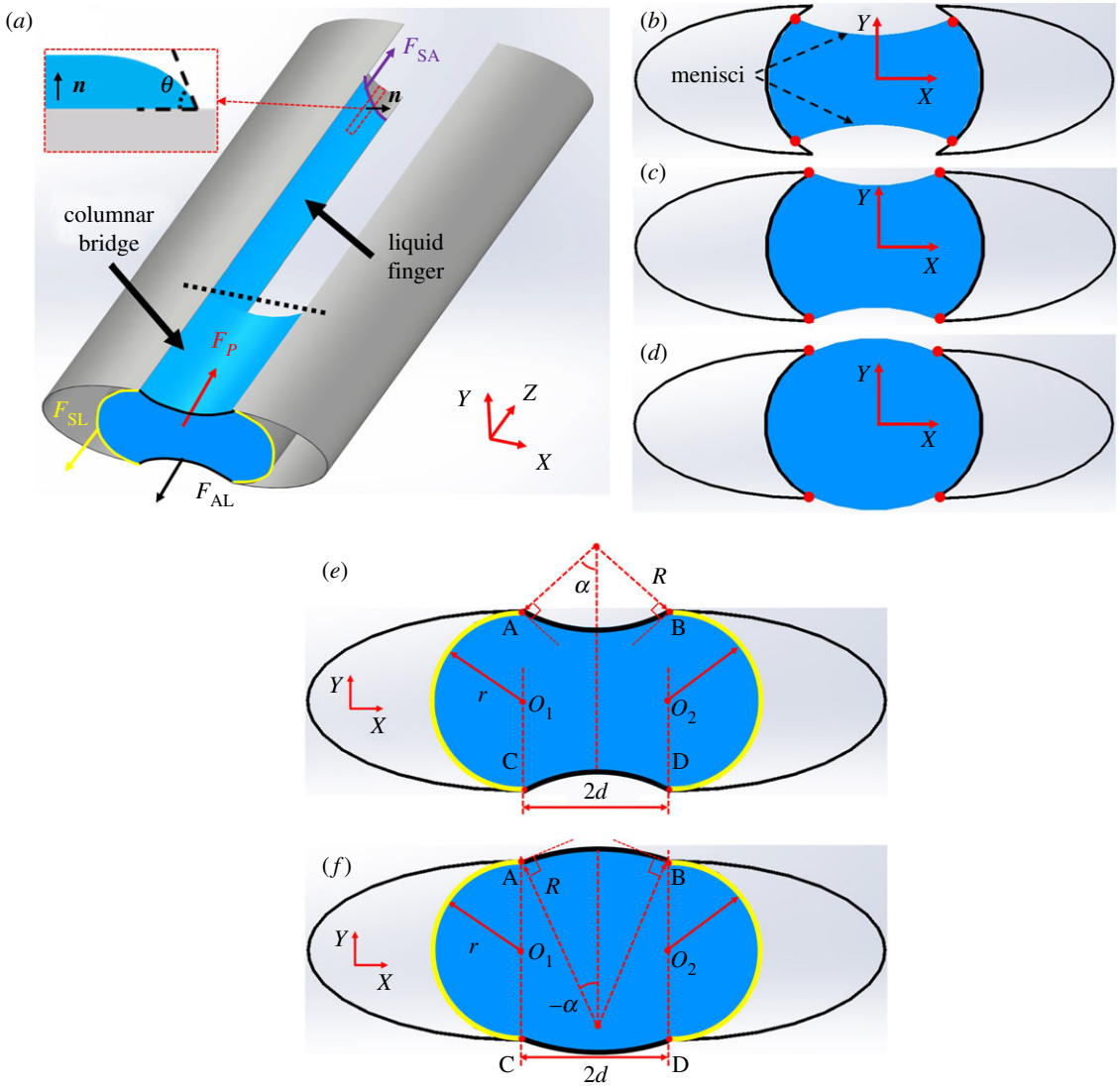

Figure 4. (*a*) A 3D schematic illustrating the shape of the columnar bridge of saliva formed between two separated galeae; the columnar bridge is in equilibrium with the liquid fingers, nucleated somewhere at the dashed line, running along the walls of each galea. The dashed box shows a cross section of the tip of the liquid finger defining the contact angle θ; the cross section is taken through a normal vector $\boldsymbol{n}$ to the food canal surface parallel to the *Z*-axis along the food canal. (*b*) Bridge cross section is perpendicular to the *Z*-axis assuming that the four contact lines (solid dots) are sitting inside the food canal. (*c*) A case of a liquid bridge with concave menisci; the bridge cross section shows four contact lines (solid dots) pinned at the legular edges of the food canal. (*d*) A case of a liquid bridge with convex menisci; the bridge cross section shows four contact lines (solid dots) pinned at the legular edges of the food canal. (*e*) Schematic of the cross-sectional shape of a saliva bridge with concave menisci connecting the two separated, parallel galeae with the contact lines pinned at the legular edges of the galeae. (*f*) Schematic of the cross-sectional shape of a saliva bridge with convex menisci. In (*e*) and (*f*), the angles formed by joining the thick solid curve and red dashed lines at points A and B are right angles, as indicated by the small red squares.

as straight parallel beams [16–18] pulled together by a force f acting per unit length of each galea (figure 4).

This capillary force is expected to scale as $f = 2\sigma u(d/r)$, where σ is the surface tension of saliva measured in Newtons per metre, $2d$ is the spacing between the two opposite legular bands of the two galeae and r is the radius of the food canal. The function $u(d/r)$ has to be identified by solving the Laplace problem of capillarity, which we discuss in detail later.

A model of a liquid column bridging two parallel, round cylindrical fibres was first discussed and analysed by Princen [16,19] and has since been widely used in different related applications [17,20–24]. Princen showed [16,19] that the mechanism of bridge break-up between the angled fibres can be revealed by analysing the behaviour of a bridge formed between two parallel fibres. We follow this model of the two parallel galeae and assume that, when the intergaleal gap reaches a certain critical value $d/r = (d/r)_{\max}$, a continuous columnar bridge breaks up, forming two fingers running along the internal C-walls of the galeae (figure 3*c*). This model of two parallel galeae with a columnar bridge sitting between them allows us to estimate the capillary force exerted on the galeae. We examine whether this force is sufficiently strong to hold the galeae together and help the insect unite the ventral legulae during proboscis assembly.

The Princen theory of bridge break-up has been designed to study the columnar bridges trapped between round cylindrical fibres, regardless of the composition of the fibres [11,16,19,21]. The galeae have a complex shape, preventing immediate application of the Princen theory to this case. We, therefore, generalize the Princen theory and study the cross-sectional profile of the columnar bridge and its effect on proboscis self-assembly.

We model the galeae as two infinitely long semi-cylinders running parallel to one another. Only the capillary force caused by the saliva bridge is considered; any pressure contribution of flow during saliva pumping is put aside and will be discussed below. Thus, the columnar saliva bridge is assumed to coexist in equilibrium with the saliva fingers running along the walls of the separated galeae (figure 4*a*). We observed that the length L of the columnar saliva bridge is much greater than the diameter of the food canal and the intergaleal separation distance $2d$.

The saliva bridge is supported by the C-face walls of the galeae, which are semicircular arcs in cross section (figure 4*a*). When the galeae are united, the food canal forms a cylindrical channel of radius r (figure 3*c*). The separation distance is denoted by $2d$ and corresponds to the distance between the two opposite legular edges of the two halves of the food canal. The inequalities $L \gg 2r$, $L \gg d$ hold true. In setting up the model, we note that the intergaleal gap, $2d$, is typically much smaller than the capillary length, based on our observations of the butterfly assembling its proboscis; thus, $l_c = \sqrt{\sigma/\rho g}$, where σ is the surface tension of saliva, ρ is the saliva density and g is the acceleration due to gravity. For water, $l_c \sim 4$ mm. This inequality, $2d \ll l_c$, implies that gravitational effects can be neglected [25]. Thus, menisci are mostly shaped by capillary forces. The meniscus meets the walls of the food canal at the contact angle θ, which is a physical parameter of the saliva–cuticle pair.

In the Cartesian system of coordinates (X, Y, Z), where the galeae are parallel to the Z-axis, the meniscus profile $Y = h(X)$ describes the liquid elevation above the reference plane $Y = 0$ (figure 4). The two menisci forming the saliva bridge are assumed to be mirror-symmetric with respect to the X-axis. As the columnar saliva bridge is connected to the saliva fingers where the pressure is constant, the pressure in the saliva bridge also has to be constant. This condition of saliva equilibrium demands that the menisci must be shaped as circular arcs to satisfy the Laplace equation of capillarity, $P = -\sigma/R$, where R is the radius of the meniscus arc. Moreover, to satisfy the condition of mechanical equilibrium of the columnar bridge/two-fingers system, the Z-component of the force acting on the system must be zero.

The force balance in the Z-direction is obtained by constructing a free-body diagram and making an imaginary cut perpendicular to the Z-axis and replacing one part of the bridge with an equivalent system of forces (figure 4*a*). At this cut, the Z-component of the force consists of five contributions: the two surface forces F_{AL} acting along the air/liquid interface, the two surface forces F_{SL} acting along the solid/liquid interface and the force F_P caused by the pressure in the saliva; this force, F_P, acts over the cross-sectional area cut. These five forces are counter-balanced by the force acting at the contact line at the end of the liquid finger, F_{SA}, and is associated with the solid/air interface. The force balance is thus written as

$$F_{AL} + F_{SL} - F_{SA} - F_P = 0. \tag{3.1}$$

To calculate the component forces, one needs to distinguish the following two scenarios of the meniscus shaping: (i) the contact lines of the menisci of the columnar bridge are sitting inside the food canal (figure 4*b*) or (ii) the contact lines are pinned at the legular edges of the food canal (figure 4*c*,*d*).

4. Analysis of possible scenarios of the saliva bridge shaping and conditions for its existence

4.1. The contact lines are sitting inside the food canal

The mathematical analysis of the force balance equation given in the electronic supplementary material shows that a long columnar bridge with the constant radius of menisci cannot be supported by the contact lines pinned to the walls of the food canal. The columnar bridge will either bulge up to form a droplet or will break up to form two separated fingers along the walls of the food canal. Thus, the case in figure 4*b* has to be eliminated from further consideration.

4.2. The contact lines are pinned at the edges of the food canal with concave menisci

The case where the liquid bridge is pinned to the edges of the food canal is special. As known from capillarity [26,27], a liquid body can form any arbitrary contact angle with a sharp edge of any corner. Therefore, the contact angle at which the meniscus meets the sharp edge of any substrate is not defined and can take on any arbitrary value. We, therefore, allow the circular arcs of the two menisci to approach the edges at any arbitrary angle. Based on figure 3*c*, the pressure inside the saliva fingers in the separated galeae with concave menisci is below atmospheric pressure. Therefore, the scenario with the convex meniscus (figure 4*d*), offering pressure in the bridge greater than atmospheric pressure, cannot support the hypothesis of a quasi-equilibrium coexistence of this bridge with the saliva fingers in the separated galeae. Thus, a discussion of convex menisci is not applicable to this case. However, the scenario of the bridge with concave menisci might be applicable.

For the concave meniscus, the parameters needed to evaluate the force balance are defined in figure 4*e*. At the reference cross section, each liquid/air interface, AB or CD, is a part of a circular cylinder of radius R with the cylinder axes parallel to the Z-axis. The position of the contact lines where the meniscus meets the galeal walls is specified by the angle α formed at the intersection of the Y-axis and the continuation of the normal vector to the meniscus surface at the edge (figure 4*e*). Thus, the central angle α completely defines the free surface of the liquid column. The arcs AC and BD are the solid/liquid interfaces and θ is the contact angle that the tip of the saliva finger makes with the galeal wall. With these notations, the force due to surface tension at the air/liquid interface is calculated as $F_{AL} = (AB + CD)\sigma$; the force due to surface tension σ_{SL} at the solid/liquid interface is $F_{SL} = \sigma_{SL}(BD + AC)$; and the force due to surface tension σ_{SA} of the solid/air interface is $F_{SA} = \sigma_{SA}(BD + AC)$. The resultant pressure acting perpendicularly to the cross-sectional area A_{ACDB} is $F_P = PA_{ACDB}$. Employing the Young–Laplace equation, $\sigma_{SA} - \sigma_{SL} = \sigma\cos\theta$ [28], we rewrite the force balance equation as

$$(AB + CD)\sigma - (BD + AC)\sigma\cos\theta - PA_{ACDB} = 0. \tag{4.1}$$

The force balance equation (4.1) is satisfied only within a limited range of contact angles θ and the ratios

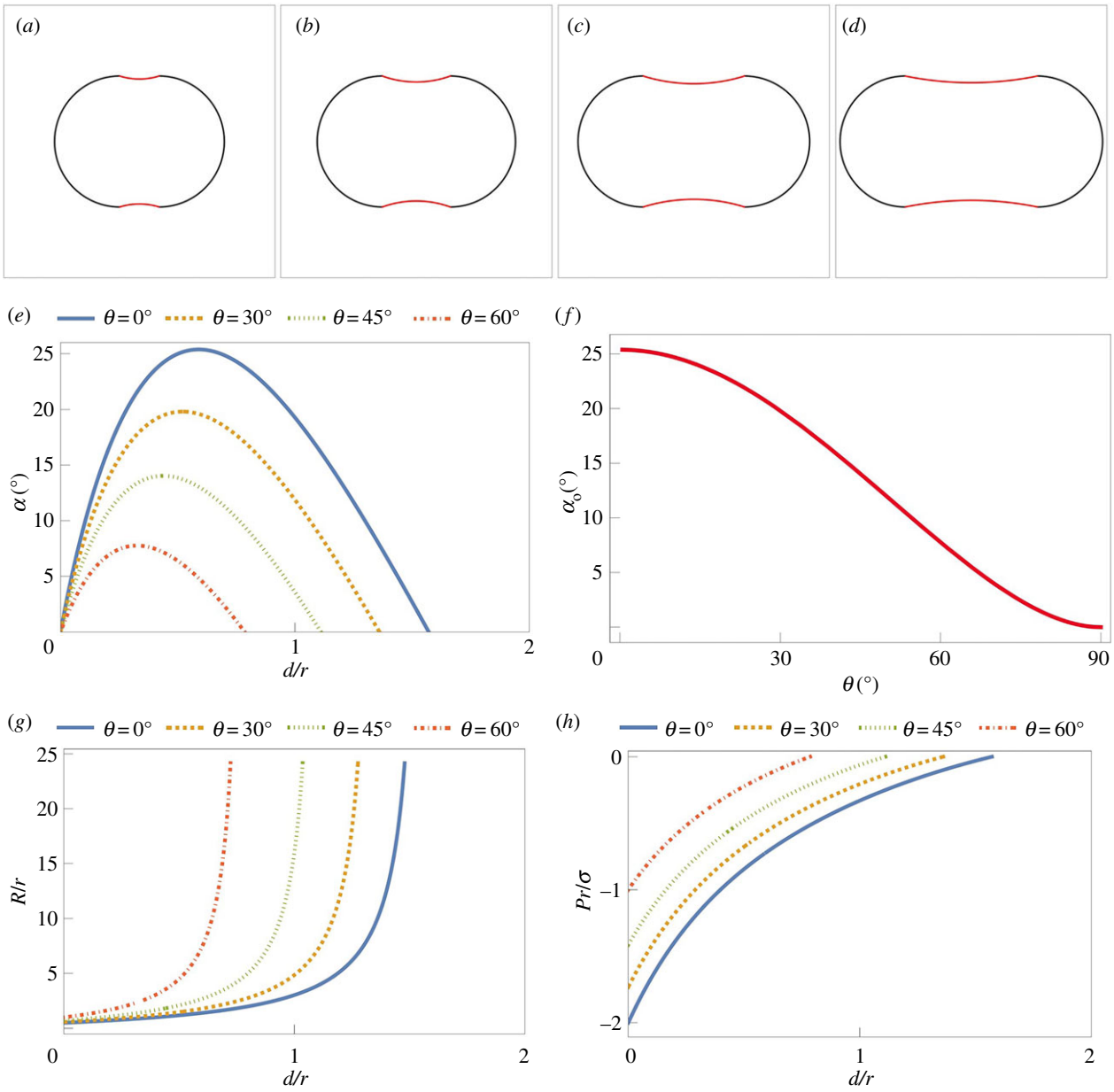

Figure 5. (*a–d*) One possible illustration of deformation of the cross-sectional profile of the saliva bridge is shown in which the intergaleal distance increases from (*a*) $d/r = 0.3$, $\alpha = 17.2^\circ$; to (*b*) $d/r = 0.52$, $\alpha = 19.8^\circ$; to (*c*) $d/r = 0.78$, $\alpha = 17.2^\circ$; and to (*d*) $d/r = 1.01$, $\alpha = 11.46^\circ$, assuming that the saliva finger makes contact angle $\theta = 30^\circ$ with the food canal cuticle corresponding to the critical meniscus arcs subtending the half-angle $\alpha_0 = 19.8^\circ$. (*e*) The angle α as a function of the dimensionless intergaleal distance d/r for different contact angles $\theta = 0^\circ$, 30°, 45°, 60°. (*f*) The maximum angle α_0 as a function of contact angle θ. (*g*) The dimensionless radius of curvature of menisci, R/r, as a function of the dimensionless intergaleal distance, d/r. (*h*) The dimensionless pressure inside the liquid meniscus, Pr/σ, as a function of the dimensionless intergaleal distance, d/r.

d/r of the intergaleal distance to the food canal diameter (electronic supplementary material). The limitation on the contact angle makes sense: the cuticle of the food canal is designed to be wettable by saliva [7], so that the contact angle should be less than 90°. The limitation on the intergaleal distance implies that lepidopterans are able to form a saliva bridge with concave menisci only when the intergaleal distance is small; that is, as the separation distance reaches a certain critical value, the bridge breaks up into two saliva fingers, confirming our observations (figure 3*c*).

Figure 5*a–d* illustrates the behaviour of the cross-sectional profile of the columnar bridge as the intergaleal distance increases. The cross-section elongates and menisci flatten; that is, their radius of curvature increases. Accordingly, suction pressure in the bridge weakens and the last term in equation (4.1) contributes less and less to the force balance as the intergaleal distance increases.

The behaviour of angle α at which menisci approach the legular edge is not monotonous (figure 5*e*). This dependence of α on the dimensionless intergaleal separation distance d/r is calculated in the electronic supplementary material. Figure 5*a–d* illustrates this non-trivial behaviour for a particular case of the contact angle $\theta = 30^\circ$. When the galeae are united, $d/r = 0$, the angle α is zero, $\alpha = 0^\circ$. When the intergaleal distance increases (figure 5*a*,*b*), the menisci develop a sag. At a certain intergaleal distance, the angle α reaches its maximum α_0. When the galeae are moved further apart, the angle α decreases (figure 5*c*,*d*). As shown in the electronic supplementary material, this maximum angle α_0

implicitly depends on the contact angle θ through the following equation:

$$\cos\theta = \frac{1}{\pi}\left[2\sin\alpha_0 + \sqrt{\pi(2\alpha_0 + \sin(2\alpha_0))}\right], \qquad (4.2)$$

and the plot of $\alpha_0(\theta)$ is presented in figure 5*f*.

Although the dependence of angle α on the intergaleal distance is non-monotonous, the radius of meniscus curvature R/r is a monotonously increasing function of the dimensionless separation distance d/r as $R/r = (d/r)/\sin\alpha$ (figure 5*g*). Accordingly, the dimensionless Laplace pressure inside the liquid meniscus, $Pr/\sigma = r/R$, increases as d/r increases (figure 5*h*).

4.3. The contact line is pinned at the edge of the food canal with convex menisci

The columnar bridge with convex menisci (figure 4*d*) cannot coexist in equilibrium with the liquid fingers forming concave menisci in the separated galeae. However, such a columnar bridge can coexist with the saliva fingers forming convex menisci; or this bridge can be formed when the insect pumps saliva and the pressure in the columnar bridge becomes greater than the atmospheric pressure. Therefore, it is instructive to analyse this scenario of equilibrium of the columnar bridge. The schematic and the geometrical parameters of this column are shown in figure 4*f*. We denote the angle as $-\alpha$, using negative to distinguish this case from the case of a concave columnar column. The force balance equation (4.1) remains the same; the relations of these forces to the geometry of convex menisci are given in the electronic supplementary material.

There is a dramatic difference in the behaviour of the angle α on the intergaleal distance d/r for convex and concave menisci (figures 6*a* and 5*e*, respectively): there are two solutions for convex menisci for each intergaleal distance d/r. As shown in [29], the more convex meniscus with the larger surface area and smaller α is unstable and hence is excluded from further analysis. As detailed in the electronic supplementary material, the boundary value of admissible angles, α, corresponding to the limit as $\mathrm{d}\alpha/\mathrm{d}(d/r) = \infty$ for any intergaleal distances d/r always equals $\alpha_c = -90^\circ$. Thus, the stable convex columnar bridges correspond to $\alpha > \alpha_c$; the columnar bridges with $\alpha < \alpha_c$ are unstable [29]. Therefore, we will consider only the cases with $\alpha > -90^\circ$.

Figure 6*b–e* illustrates the behaviour of the cross-sectional profile of the convex columnar bridge as the intergaleal distance increases, $\alpha > -90^\circ$. The radius of meniscus curvature R/r and the dimensionless Laplace pressure $Pr/\sigma = r/R$ inside the columnar bridges are plotted as a function of the intergaleal distance d/r in figure 6*f*,*g*, respectively.

The angle α monotonously decreases from zero to -90° with the increasing intergaleal distance d/r (figure 6*a*), the cross-section elongates and the menisci bulge (i.e. their radius of curvature decreases, figure 6*f*). Accordingly, the repulsive pressure in the bridge increases (figure 6*g*), and the last term in equation (4.1) contributes more and more to the force balance as the intergaleal distance increases.

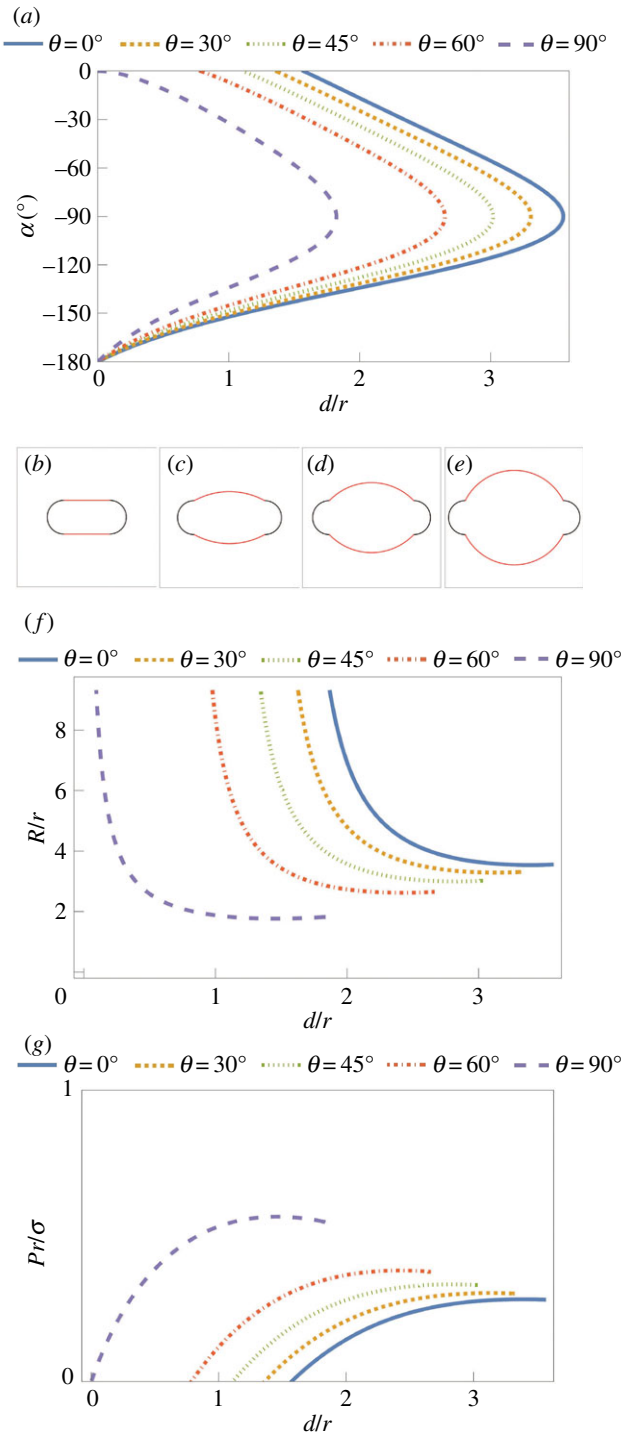

Figure 6. (*a*) The angle α as a function of the dimensionless intergaleal distance d/r for different contact angles $\theta = 0^\circ$, 30°, 45°, 60°, 90°. (*b–e*) Illustrations of deformation of the cross-sectional profile of the columnar bridge when the intergaleal distance increases from (*b*) $d/r = 1.36$, $\alpha = 0^\circ$; to (*c*) $d/r = 2.1$, $\alpha = -28.6^\circ$; to (*d*) $d/r = 2.54$, $\alpha = -45.8^\circ$; and to (*e*) $d/r = 2.95$, $\alpha = -63^\circ$, assuming that the liquid finger makes contact angle $\theta = 30^\circ$ with the food canal. (*f*) The dimensionless radius of curvature of menisci, R/r, as a function of the dimensionless intergaleal distance, d/r. (*g*) The dimensionless pressure, Pr/σ, inside the liquid meniscus as a function of the dimensionless intergaleal distance, d/r.

5. The capillary force exerted on the galeae

Considering the force per unit length of the galea f (i.e. force density), we can evaluate it using a free-body diagram (figure 7*a*). An imaginary cut is made along the columnar bridge, the dashed line. The obtained cross section of this column along the tube axis is a curved rectangle: two sides of the rectangle are straight lines running parallel to the proboscis axis Z, the side that belongs to the frontal meniscus is curved, and the opposite side that ends somewhere near the

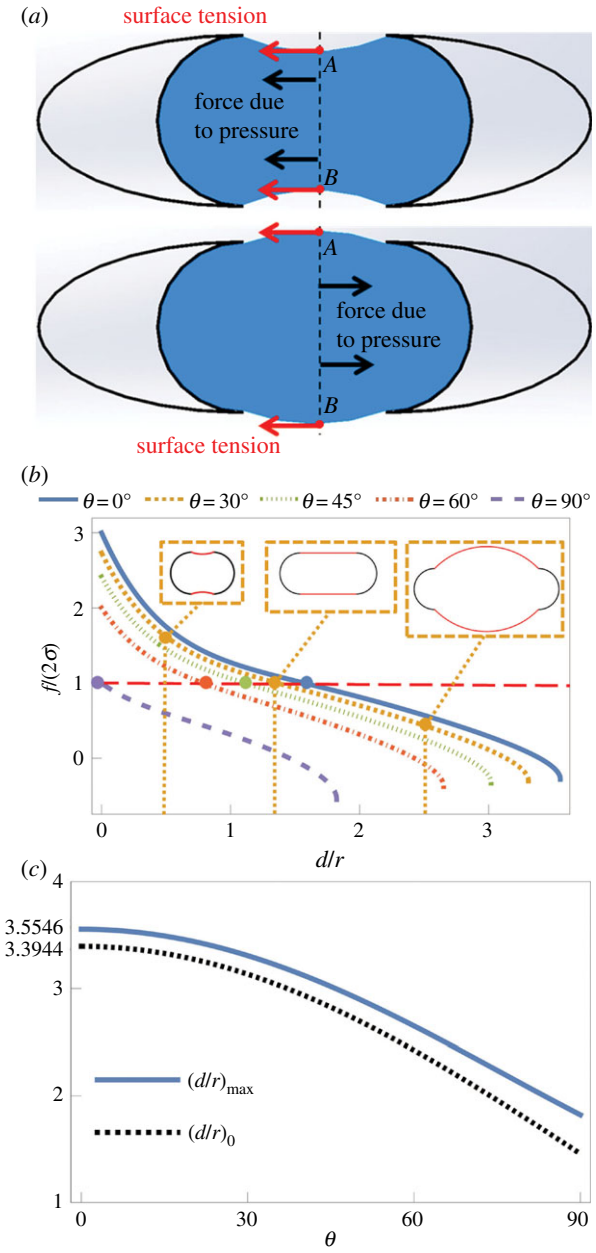

Figure 7. (*a*) Schematic illustrating the force analysis on concave and convex liquid bridges. (*b*) The normalized intergaleal force $f/(2\sigma)$ as a function of normalized intergaleal distance d/r at different contact angles $\theta = 0^\circ$, 30°, 45°, 60°, 90° for all scenarios. The red dashed line and the solid dots separate the concave (above) and the convex (below) columnar bridges. The meniscus profiles in the dashed boxes correspond to $\theta = 30^\circ$ and different intergaleal distances. (*c*) The maximum intergaleal distance $(d/r)_{max}$ below which a columnar bridge can exist and the intergaleal distance $(d/r)_0$ at which the intergaleal force goes to zero. They depend only on the contact angle.

base of the proboscis may be curved as well. We remove the left side of the column and introduce an equivalent system of forces to support the remaining part of the column in equilibrium. When the column is much longer than the diameter of the food canal, the contribution to the force balance of the two curved sides at the ends of this cut is negligibly small and we can neglect this contribution. Thus, the capillary force exerted by the columnar bridge on the unit length of the galea consists of the two components: the surface tension component and pressure component,

$$f = 2\sigma - P \cdot \overline{AB}, \tag{5.1}$$

where the first term on the right-hand side, $2\sigma \cdot 1$, is the tension on the two surfaces along the unit length of the A and B sides of the curved rectangle; the second term is the product of the cross-sectional area $\overline{AB} \cdot 1$ and pressure $P = \mp\sigma/R$ in the saliva bridge for concave and convex columnar bridges, respectively.

Substituting into equation (5.1), the relations $\overline{AB} = 2r \mp 2(R - R\cos\alpha)$, $d = \pm R\sin\alpha$, for concave and convex columnar bridges, respectively, we obtain

$$f = 2\sigma \pm \frac{\sigma}{R}[2r \mp 2(R - R\cos\alpha)] = 2\sigma\left(\cos\alpha + \frac{\sin\alpha}{d/r}\right). \tag{5.2}$$

It is convenient to introduce a scale for the capillary force f as 2σ. We show the dependence of the dimensionless force $f/(2\sigma)$ on the ratio d/r for different contact angles θ for both concave and convex cases (figure 7*b*). The force f is always positive for concave columnar bridges, which means it always pulls the two separated galeae together. Indeed, the surface tension acts to contract the air/liquid surface, tending to bring the galeae together. In addition, concave menisci generate a suction capillary pressure that adds to the surface tension pull of the galeae together. Convex columnar bridges also experience the surface tension pulling the galeae together. However, the capillary pressure of convex columnar bridges is greater than atmospheric pressure; hence, the pressure in these bridges always pushes the galeae to spread apart. Figure 7*b* reveals a surprising effect: when the surface tension remains greater than the pressure acting over the galeal surfaces, some convex columnar bridges can be pulled together.

Based on our experimental observations of monarch butterflies and painted lady butterflies [30], the columnar bridge breaks up to form the two separated saliva fingers when $d/r \approx 0.5$, and the contact angle between saliva and the food canal is close to 0°. Examination of the curves in figure 7*b* suggests that, within this region, the force $f/(2\sigma)$ decreases almost linearly with d/r. Thus, approximation of the force in the form

$$\frac{f}{2\sigma} = a \cdot \frac{d}{r} + b \tag{5.3}$$

is attractive due to its simplicity. In the linear approximation, equation (5.3), the constants a and b are considered parametrically dependent on the contact angle θ: $a = -2.26 \cdot \cos\theta - 0.98$ and $b = 1.98 \cdot \cos\theta + 0.96$. In the electronic supplementary material, we provide details of the analysis of this approximation and show that approximation (5.3) is valid for contact angles less than 90°.

For each contact angle θ, the maximum capillary force corresponds to the united proboscis. As the intergaleal distance increases, the capillary attraction between the galeae decreases.

The convex columnar bridge can exist only when the galeae are separated (figure 6): the limiting case of the 90° contact angle is an exception. In this case, the galeae are united, no fingers form ahead of the columnar liquid bridge in figures 3 and 4, and the frontal meniscus is flat, approaching the walls of the food canal at the 90° contact angle. As soon as the contact angle decreases, the galeae have to be separated to make the columnar bridge with the convex profile stable. The frontal meniscus takes on a complex saddle-like shape to satisfy the Laplace equation of capillarity and contact angle restriction. For example, for

the zero contact angle, the galeae supporting a columnar bridge have to be spread apart for the distance larger than the radius of the food canal.

Comparison of figures 6*g* and 7*c* shows that stable menisci can be found at distances greater than $(d/r)_0$. The reason for this is that the developed model describes liquid columns formed between fixed galeae; the intergaeal distance in that case can be varied up to $(d/r)_{max} > (d/r)_0$ and the columnar bridge is expected to remain stable up to $(d/r)_{max}$. By contrast, when the galeae are free to move, at point $(d/r)_0$, the total force flips from the attractive to repulsive, pushing the galeae to spread apart; thus, the criterion for galeal assembly by capillary action of a saliva column is $(d/r) < (d/r)_0$.

The limiting case as the intergaleal separation goes to zero, $d/r \to 0$, deserves special attention. This limit describes a united proboscis where the pressure in the liquid column is set up by the spherically capped frontal meniscus, which meets the wall of the food canal at the contact angle θ. Therefore, the pressure in the column becomes $P = -2\sigma\cos\theta/r$. The area of this rectangular cross section of a column of unit length is $\overline{AB} = 2r \cdot 1$. Therefore, the force per unit length acting on the galea is $f = 2\sigma - P \cdot \overline{AB} = 2\sigma + 4\sigma\cos\theta$. This force is the upper limit for the capillary force exerted by the columnar bridge of saliva on the galeae. Taking $\theta = 0^\circ$, we find $f_{max} = 6\sigma$. Thus, in the limiting case as the galeae come together, the frontal meniscus significantly contributes to the force by increasing it threefold!

An order of magnitude estimate of the galeal deflection due to the capillary force can be done using equation (5.3): in the unloaded case, when the columnar bridge is absent, the force is zero. Therefore, the capillary force is expected to provide deflection of the order of $(d/r) \simeq b/a$. Our experimental observations on monarch butterflies and painted lady butterflies [30] support this order of magnitude estimate, showing that the columnar bridge breaks up to form the two separated saliva fingers when $d/r \approx 0.5$ (i.e. of the order of 1).

As follows from this analysis, the longer the columnar bridge, the greater the force it exerts on the galeae. Thus, it is plausible that the galeae can be held in close contact, $\ll r$, by the capillary force while the insect works to couple the legulae.

Figure 7*b* shows that the force remains attractive even if the meniscus becomes convex. Thus, the capillary attraction of galeae wetted by saliva is expected to show up not only in static cases when the pressure in the columnar bridge is below atmospheric, but also in some dynamic cases when the insect pumps saliva into the intergaleal gap, increasing the pressure above atmospheric pressure. To examine this possibility, we used an artificial proboscis.

6. Assembly of artificial proboscis

6.1. Columnar bridges with concave meniscus

To further demonstrate the effect of capillary force from the saliva column on the self-assembly of the lepidopteran proboscis, the following physical model was constructed and studied experimentally. A 3M® polyolefin (poly(ethylene-co-vinyl acetate)) tube with a 2.2 mm outer diameter and 1.1 mm inner diameter was chosen to be about the same size as the hawk moth proboscis. The tube was partially cut along its axis. Young's modulus of these tubes, $E = 60$ MPa, measured on an Instron machine is greater than or

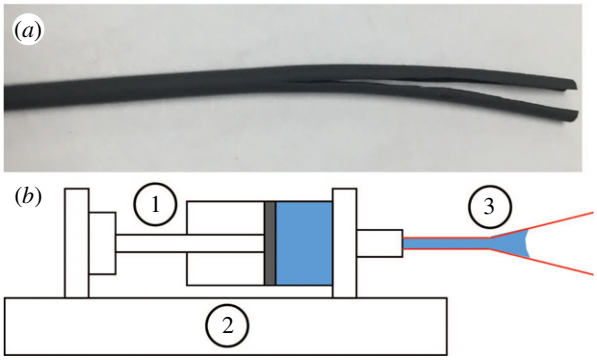

Figure 8. (*a*) Polyolefin tube partially cut along its axis. (*b*) Schematic of set-up modelling the proboscis self-assembly. The partially cut tube (3) is connected to a syringe filled with the wetting (blue) liquid (1) and placed on a syringe pump (2).

comparable to our measurements of lepidopteran proboscises. The artificial proboscis consisted of a cylindrical tube with two half-tubes at one end. The tubular part was connected to a syringe filled with hexadecane forming a zero contact angle with the tube. We chose hexadecane, a completely wetting fluid, to remove any effect of contact angle; it possibly mimics the effect of saliva, which presumably completely wets the food canal [7,31]. Water provides the other limiting case by giving a contact angle of 90°. The syringe with the attached artificial proboscis was placed on a syringe pump (New Era Pump Systems, Inc.; NE-300) (figure 8). During the experiment, hexadecane, which has a contact angle of 0° with the tube, was pumped through the tube, and the response of the separated half-tubes was recorded with a Redlake MotionPro X3 camera with a microscopic lens (Meiji Techno® Short UNIMAC MacroZoom Lense MS-40) at a 30 fps frame rate. In this experiment, only capillary forces were expected to bring the separated half-tubes together; no other forces were involved. Thus, this set-up models the effect of the capillary action of saliva while excluding the effect of muscular action in the galeae and any behaviours of the butterfly.

Two sets of experiments were conducted with this set-up. In the first set, the liquid was pumped continuously through the tube at a constant rate of 0.1 ml min^{-1}. The response of the artificial galeae was recorded (figure 9). At the beginning of the experiment, the two halves were separated (figure 9*a*). In this example, the half-tubes remained almost parallel to one another with a small in-plane spontaneous curvature acquired by each half after cutting the whole tube.

When the meniscus reached the region of observation from the bottom (figure 9*b*), it brought the two halves closer: the gap between them (figure 9*b*) decreased relative to that in figure 9*a*. The two halves nearly connected behind the frontal meniscus while they remained separated ahead of it. We also observed this effect in live monarch butterflies.

As the pumping continued, the meniscus front, highlighted in the blue dashed box (figure 9*b*,*c*), moved towards the top of these frames and then left the frame. The thickness of the air gap visibly decreased and finally disappeared (figure 9*d*,*e*): the two halves came together to form a united artificial food canal. No other forces acted on the separated halves; thus, we can conclude that it was the capillary force from the hexadecane meniscus that brought the halves together.

In the second set of experiments, the meniscus was moved beyond the area of observation and then the pump

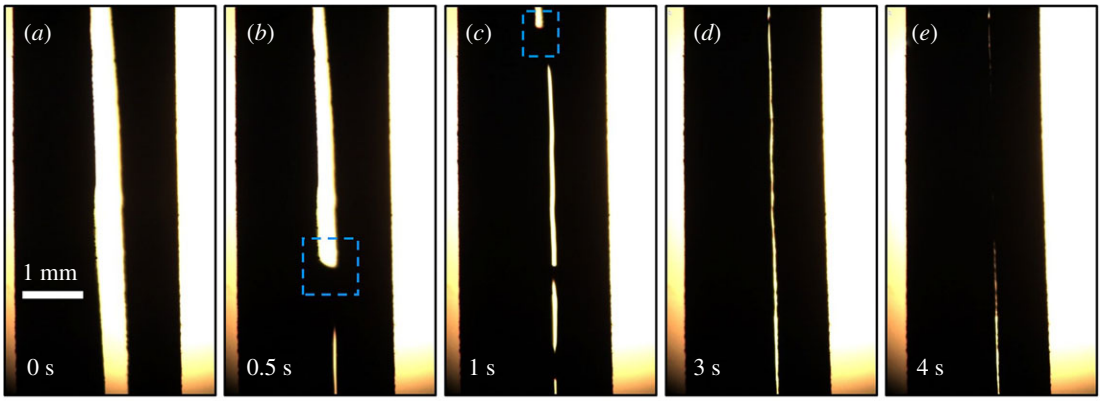

Figure 9. (*a*) The two dark half-tubes modelling the galeae are separated by an air gap; the tube base (bottom of image) and two halves are empty. (*b*,*c*) When hexadecane is pumped through the tube base and fills the gap between the artificial galeae, the frontal meniscus boxed by the dashed lines moves forward (i.e. towards the top of the image) and the columnar bridge left behind this meniscus pulls the artificial galeae together. (*d*,*e*) When the meniscus advances, the capillary force exerted by the columnar bridge gets stronger, bringing the artificial galeae in direct contact with one another.

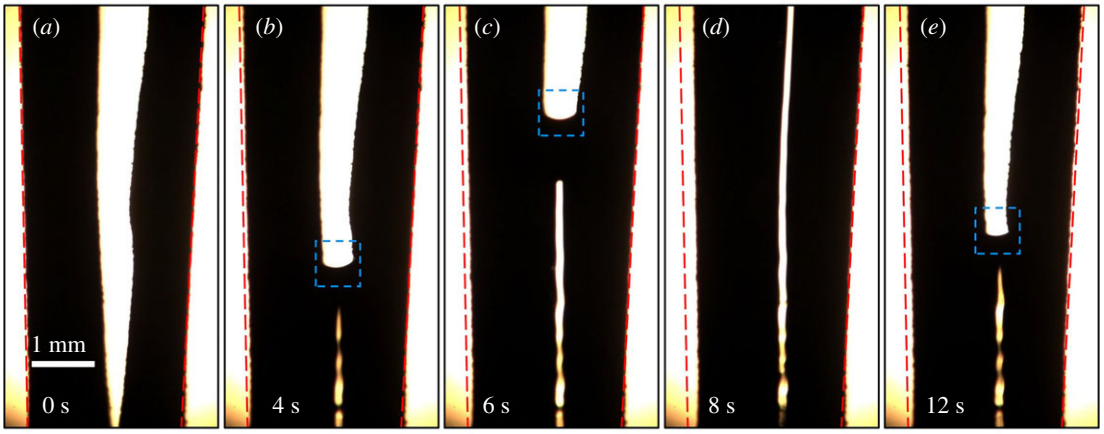

Figure 10. (*a*) Before hexadecane pumping, the two dark half-tubes modelling the galeae are separated by an air gap; the dashed borders are shown for reference to measure deflections of the half-tubes. (*b*–*d*) When hexadecane is pumped through the base tube and fills the artificial galeae, the frontal meniscus boxed by the dashed lines moves forward and the columnar bridge left behind this meniscus pulls the artificial galeae together. (*e*) The meniscus retracts after stopping the pump. This frame shows an equilibrium configuration of the half-tubes and the remaining columnar liquid bridge holding the half-tubes in close contact.

was stopped (i.e. the piston in the pumping syringe was stopped). Thus, the hexadecane had no room to flow back to the syringe. The behaviour of the separated half-tubes is illustrated with a sequence of frames in figure 10. In the reference (figure 10*a*), we show the shape of the two separated half-tubes in the region of observation before hexadecane pumping when they were completely empty. The red dashed lines mark the original position of each half, and are used to determine the displacement caused by the capillary forces. In this example, the right half-tube acquired a larger spontaneous radius of curvature after cutting the whole tube in half. Therefore, the right half is stiffer and difficult to deform. The left half has a small spontaneous curvature and, hence, is easier to deform.

During pumping, the meniscus moved from the bottom to the top of these frames, causing the left half-tube to move closer to the right stiffer half-tube. The left half moved closer and closer to the right half-tube away from the reference marker while the right stiff half-tube remained almost undeformed (figure 10*b*–*d*). When the pump was stopped, we observed the meniscus retracting. Figure 10*e* depicts the equilibrium position of the meniscus after it has moved back. In the equilibrium state, the gap between the two half-tubes is larger than the case when these halves were bridged by the columnar menisci in figure 10*d*, but the left half-tube remains deflected from the original configuration in figure 10*a*. This deflection is caused by capillary forces acting along the remaining columnar liquid bridge.

The hexadecane had no room to flow back to the syringe; therefore, meniscus retraction was caused by two forces: the surface forces that tend to decrease the surface area of the columnar liquid bridge and the wetting forces that pull the columnar bridge forward, forcing the hexadecane to cover the surfaces of the half-tubes. The capillary force holding the two halves together decreased as the distance between the half-tubes increased (figure 7*b*). Therefore, when the pump stopped, some liquid moved to the liquid fingers present in the separated half-tubes. This flow resulted in meniscus retraction and simultaneous deflection of the left half-tube. The flow continued until the wetting and capillary forces of the columnar bridge were counterbalanced by the elastic force from the half-tubes. This phenomenon qualitatively mimics the observed self-assembly process of the lepdiopteran proboscis.

6.2. Columnar bridges with convex meniscus

The model predicts that the convex saliva meniscus can create an attractive force, given that muscular contraction

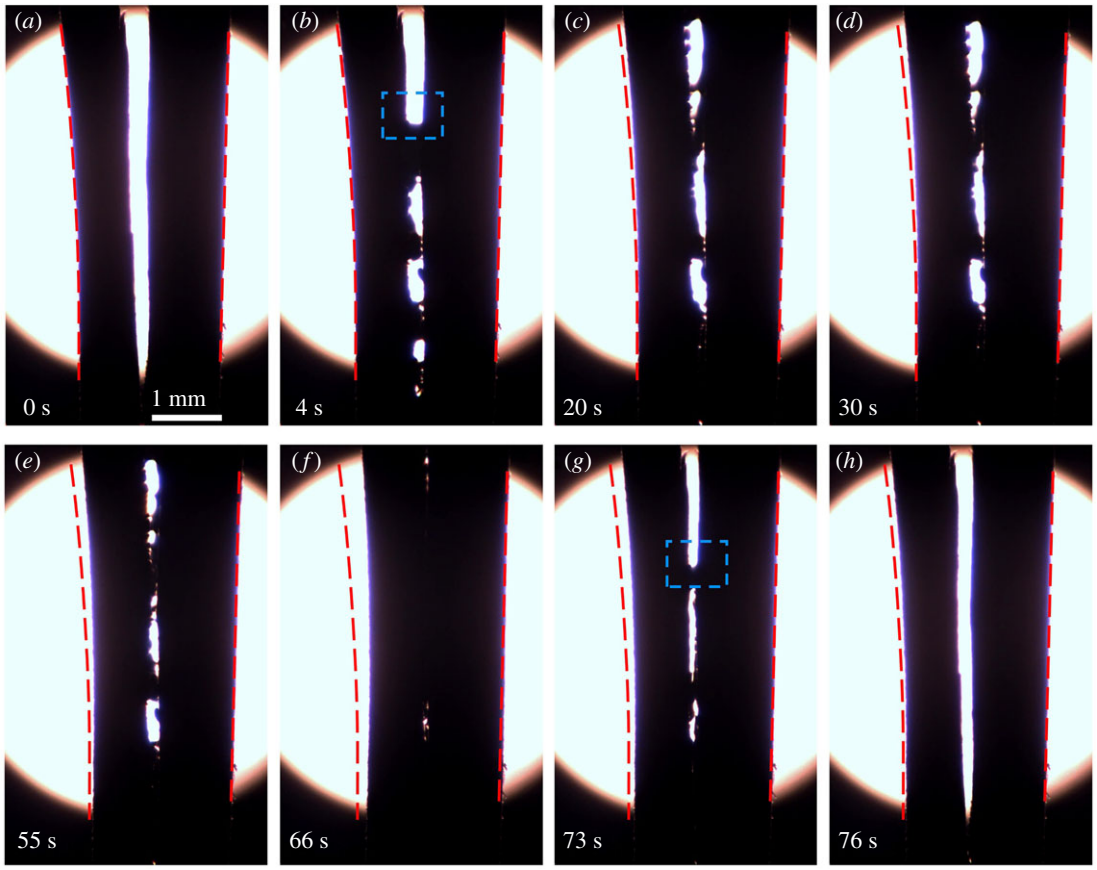

Figure 11. (*a*) Before water pumping, the two dark half-tubes modelling the galeae are separated by an air gap; the dashed borders are shown for reference to measure deflections of the half-tubes. (*b–d*) When water is pumped through the tube base and fills the artificial galeae, the frontal meniscus, boxed by the dashed lines, moves forward and the columnar bridge left behind this meniscus pulls the artificial galeae together. (*e–h*) The meniscus retracts after changing from pumping to withdrawing. (*e,f*) The artificial galeae draw closer and closer after removing liquid from the meniscus by decreasing pressure in the column. (*g,h*) The artificial galeae are further separated after shortening and complete removal of the columnar bridge.

and lepidopteran behaviours are absent, at some range of separation d/r (figure 7*c*). This result is counterintuitive: the Laplace pressure in the columnar bridge is larger than atmospheric pressure; therefore, one would argue that the galeae should tend to separate. However, the surface tension of the columnar bridge always pulls the separated galeae together, counterbalancing the pressure within some range of intergaleal gaps.

To check this result experimentally, we used a non-wetting liquid. Our capillary rise experiments showed that water forms $\theta = 90^\circ$ with the 3M® polyolefin tubes. This contact angle guarantees formation of a columnar bridge with a convex meniscus (figures 6 and 7); moreover, at small intergaleal distances $d/r < 1$, this columnar bridge should exert an attractive capillary force that pulls the artificial galeae together. Thus, water, which is similar to the nearly inviscid saliva, provides an opportunity to test our hypothesis that the columnar bridge with a convex meniscus can create an attractive force.

We conducted the following experiments to test this hypothesis. First, water was pumped for 20 s through the artificial proboscis (figure 11*a–c*). When the water meniscus arrived at the bifurcation (figure 11*b*), the deflection of the two halves was negligible compared with their initial configurations. After 20 s of pumping when the water meniscus passed the observation area to form a long columnar bridge (figure 11*c*), a noticeable deflection of the left half was observed. This deflection remained almost unchanged after pumping for 20 more seconds, that is, when the water meniscus travelled about twice the distance to form the twice-longer columnar bridge. In contrast with the case of complete wetting of the artificial proboscis with hexadecane (figure 9), the free halves did not unite completely (figure 11*d*). This observation confirmed that the attractive capillary force is weaker than that of the wetting fluid, in full accord with theoretical predictions (figure 7*b*).

After pumping for 40 s, the pump was reversed to withdraw water from the artificial proboscis. Thus, the pressure in the columnar bridge decreased with respect to atmospheric pressure. An appreciable change in deflection of the left half-tube became apparent after 15 s of water withdrawal (i.e. at 55 s; figure 11*e*). After 11 more seconds, the two half-tubes united (figure 11*f*). When the water meniscus retracted to the observation area, the two half-tubes spread apart (figure 11*g*), and finally returned to the initial configuration when the water meniscus disappeared from the area of observation (figure 11*h*). These two series of experiments confirmed the capillary attraction hypothesis for proboscis assembly.

7. Discussion and conclusion

Proboscis self-assembly is an integrated behavioural and mechanical process involving galeal musculature, palpal manipulations, legular coupling, and repeated coiling and uncoiling of the proboscis [5]; we are addressing the role of these factors in ongoing experiments. Our focus here has been to isolate the passive forces involved in self-assembly. The routine discharge of saliva during proboscis assembly suggested our working hypothesis: Lepidoptera unite their galeae with the aid of

capillary attraction by saliva. Our earlier analysis of saliva viscosity suggests that it lacks sliminess (i.e. viscoelasticity) and behaves like a simple, water-like Newtonian fluid [10].

X-ray micro-CT of freshly killed insects helped us identify the behaviour of a wetting fluid inside partially separated galeae. We showed that, when the intergaleal gap is small, a long columnar liquid bridge forms. The column terminates in two liquid fingers situated in the separated galeae. Consequently, we formulated a model based on our observations that saliva forms a column bridging the two galeae by capillary action. A theoretical investigation of the criteria for existence of these columns and the analysis of capillary forces exerted on the galeae revealed a set of plausible scenarios for passively holding the galeae together while the insect couples the ventral legulae to mechanically hold the galeae in place. We discovered that capillary attraction can be realized when capillary Laplace pressure of the wetting fluid is (i) lower than atmospheric pressure (i.e. the static case when the columnar bridge causes galeal attraction by suction effect) and (ii) greater than atmospheric pressure (i.e. the dynamic case when surface tension pulls the galeae together but pressure pushes them apart). We confirmed our theoretical analysis with a series of illustrative experiments on artificial proboscises made of polyolefin tubes.

The often-copious production of saliva and its energy-conserving (passive) role in proboscis assembly suggest that a well-hydrated insect is critical to successful proboscis assembly. Small animals are highly susceptible to loss of body water as a function of their small size and the consequent high surface area-to-volume ratio [32]. We periodically have observed lepidopterans in our colonies that have deformed wings and proboscises that remain uncoupled and distally withered, particularly under dry rearing conditions. We have shown that Lepidoptera can conserve fluids, including saliva, by bending and coiling the proboscis [13]. When saliva is alternately pumped into and retracted from the food canal, water could be lost to evaporation, especially in diurnal Lepidoptera exposed to the sun. Bending and coiling the proboscis during assembly, however, facilitate fluid collection at the permeable dorsal and ventral legular bands [13]. Movement of fluid to the legular bands would promote not only capillary attraction but also re-entry of the fluid into the food canal, thus counteracting any tendency for fluid to remain on the larger evaporative surface of the outer galeal walls.

Because saliva serves as an attractive force for holding the galeae together, we suspect that the act of imbibing fluids not only benefits water balance and nutritional needs, but also facilitates galeal attraction. We suggest, therefore, that the act of fluid feeding would conserve saliva and help ensure that the galeae remain coupled despite mechanical stresses encountered during vigorous probing of a food source (e.g. floral corollas), bending and pressing the proboscis against a substrate (e.g. fig. 3 in [33]) and lateral sweeping of the proboscis over a substrate (e.g. decaying fruit [34]).

Lepidopteran saliva solubilizes encrusted sugars, other non-fluid nutriment and highly viscous nectar [33,34]. We have previously shown, however, that the viscosity of lepidopteran saliva does not differ significantly from the viscosity of nectar that butterflies typically imbibe. The role of saliva in rendering most nectars (i.e. up to 40% sugar solutions) used by Lepidoptera less viscous, therefore, would be minimal [3]. The principal functions of saliva for most adult Lepidoptera with a coilable proboscis would seem to be nutrient solubilization and galeal attraction during proboscis assembly. The unique pollen-gathering butterflies (e.g. certain *Heliconius* species) use saliva for processing the pollen for its constitutive nutrients [35]. Saliva in adult Lepidoptera also might serve as (i) a medium for extra-oral delivery of enzymes, such as invertases [36], and, in more restricted cases, proteases [37], (ii) a lubricant in antiparallel movements of the galeae after assembly, and (iii) a medium for dislodging debris and self-cleaning the proboscis.

The role of saliva in self-assembly allows testable predictions about the relative production of saliva and development of the salivary glands across the Lepidoptera. Moths with a proboscis too short to coil typically do not couple their galeae, or do so only weakly [33,38]. Ancient lepidopteran lineages, such as the Eriocraniidae, do not even couple the galeae during liquid uptake [39]. If proboscis assembly of these insects is minimal or absent, we would expect the role of saliva during assembly to be correspondingly minimal. Thus, these moths should have salivary glands less developed, *ceteris paribus*, than those of species with fully coilable proboscises that require assembly. The family Notodontidae offers an attractive opportunity for testing this hypothesis through behavioural studies of proboscis manipulation at eclosion from the pupa and comparative anatomical analyses of the salivary glands. The family includes representatives with short uncoilable organs and long coilable proboscises, as well as intermediates with at least partially coilable organs mechanically coupled by ventral legulae [39,40].

Data accessibility. All experimental data have been included in the manuscript. Data for the model analysis, linear approximation of the capillary force and the image analysis have been included in the electronic supplementary material.

Authors' contributions. P.H.A. and K.G.K. conceived the project and wrote the paper. K.G.K. designed the experiments and constructed the model. C.Z. conducted all X-ray micro-CT and artificial proboscis experiments and conducted numerical analysis of the model. D.M. and T.A. filmed the butterfly emergence from the pupa and documented continuous saliva discharge. C.E.B. and S.P. established insect colonies and provided all living material for experimentation. C.E.B. provided scanning electron micrographs and participated in the X-ray micro-CT imaging. All authors gave final approval for this publication.

Competing interests. We declare we have no competing interests.

Funding. This work was supported in part by National Science Foundation awards POL-S1305338, IOS-1354956, and the SC EPSCoR/IDeA Program under NSF Award no. OIA-1655740. The views, perspective, and content do not necessarily represent the official views of the SC EPSCoR/IDeA Program nor those of the NSF.

Acknowledgements. We thank Golnaz Najaf Tomaraei for her help with the model analysis, John Udall for donating the OMNIPAQUE and the Clemson University Electron Microscope Facility for providing scanning electron microscope time and assistance.

References

1. Eastham LES, Eassa YEE. 1955 The feeding mechanism of the butterfly *Pieris brassicae* L. *Phil. Trans. R. Soc. B* **239**, 1–43. (doi:10.1098/rstb.1955.0005)

2. Snodgrass RE. 1961 The caterpillar and the butterfly. *Smithson. Misc. Coll.* **143**, 1–51.

3. Krenn HW. 2010 Feeding mechanisms of adult Lepidoptera: structure, function, and evolution of the mouthparts. *Annu. Rev. Entomol.* **55**, 307–327. (doi:10.1146/annurev-ento-112408-085338)
4. Wigglesworth VB. 1972 *The life of insects*, 3rd edn. New York, NY: Weidenfeld and Nicolson.
5. Krenn HW. 1997 Proboscis assembly in butterflies (Lepidoptera)—a once in a lifetime sequence of events. *Eur. J. Entomol.* **94**, 495–501.
6. Davis NT, Hildebrand JG. 2006 Neuroanatomy of the sucking pump of the moth, *Manduca sexta* (Sphingidae, Lepidoptera). *Arthropod. Struct. Dev.* **35**, 15–33. (doi:10.1016/j.asd.2005.07.001)
7. Monaenkova D, Lehnert MS, Andrukh T, Beard CE, Rubin B, Tokarev A, Lee WK, Adler PH, Kornev KG. 2012 Butterfly proboscis: combining a drinking straw with a nanosponge facilitated diversification of feeding habits. *J. R Soc. Interface* **9**, 720–726. (doi:10.1098/rsif.2011.0392)
8. Tsai CC, Monaenkova D, Beard CE, Adler PH, Kornev KG. 2014 Paradox of the drinking-straw model of the butterfly proboscis. *J. Exp. Biol.* **217**, 2130–2138. (doi:10.1242/jeb.097998)
9. Krenn HW, Muhlberger N. 2002 Groundplan anatomy of the proboscis of butterflies (Papilionoidea, Lepidoptera). *Zool. Anz.* **241**, 369–380. (doi:10.1078/0044-5231-00078)
10. Tokarev A, Kaufman B, Gu Y, Andrukh T, Adler PH, Kornev KG. 2013 Probing viscosity of nanoliter droplets of butterfly saliva by magnetic rotational spectroscopy. *Appl. Phys. Lett.* **102**, 033701. (doi:10.1063/1.4788927)
11. Bico J, Roman B, Moulin L, Boudaoud A. 2004 Elastocapillary coalescence in wet hair. *Nature* **432**, 690. (doi:10.1038/432690a)
12. Lehnert MS, Monaenkova D, Andrukh T, Beard CE, Adler PH, Kornev KG. 2013 Hydrophobic–hydrophilic dichotomy of the butterfly proboscis. *J. R Soc. Interface* **10**, 20130336. (doi:10.1098/rsif.2013.0336)
13. Zhang C, Beard CE, Adler PH, Kornev KG. 2018 Effect of curvature on wetting and dewetting of proboscises of butterflies and moths. *R. Soc. open sci.* **5**, 171241. (doi:10.1098/rsos.171241)
14. Hepburn HR. 1971 Proboscis extension and recoil in Lepidoptera. *J. Insect Physiol.* **17**, 637–656. (doi:10.1016/0022-1910(71)90114-4)
15. Pometto S. 2014 Repair of the proboscis of brush-footed butterflies (Lepidoptera: Nymphalidae). Master's thesis, Clemson University, Clemson, SC, USA.
16. Princen HM. 1970 Contact angles from capillary rise between filaments in a V-configuration. *Text. Res. J.* **40**, 1069–1072. (doi:10.1177/004051757004001204)
17. Soleimani M, Hill RJ, van de Ven TGM. 2015 Capillary force between flexible filaments. *Langmuir* **31**, 8328–8334. (doi:10.1021/acs.langmuir.5b01351)
18. Sauret A, Boulogne F, Somszor K, Dressaire E, Stone HA. 2017 Drop morphologies on flexible fibers: influence of elastocapillary effects. *Soft Matter* **13**, 134–140. (doi:10.1039/c6sm00921b)
19. Princen HM. 1970 Capillary phenomena in assemblies of parallel cylinders: III. Liquid columns between horizontal parallel cylinders. *J. Colloid. Interf. Sci.* **34**, 171–184. (doi:10.1016/0021-9797(70)90167-0)
20. Keis K, Kornev KG, Kamath YK, Neimark AV. 2004 Towards fiber-based micro- and nanofluidics. In *Nato Sci Ser II math*, pp. 175–182. Dordrecht, The Netherlands: Kluwer Publishing.
21. Duprat C, Protière S, Beebe AY, Stone HA. 2012 Wetting of flexible fibre arrays. *Nature* **482**, 510–513. (doi:10.1038/nature10779)
22. Liu JL, Feng XQ. 2012 On elastocapillarity: a review. *Acta Mech. Sin.* **28**, 928–940. (doi:10.1007/s10409-012-0131-6)
23. Boulogne F, Sauret A, Soh B, Dressaire E, Stone HA. 2015 Mechanical tuning of the evaporation rate of liquid on crossed fibers. *Langmuir* **31**, 3094–3100. (doi:10.1021/la5050361)
24. Duprat C, Stone HA. 2016 Elastocapillarity. In *Fluid-structure interactions in low-Reynolds-number flows* (eds C Duprat, H Stone), pp. 193–246. Cambridge, MA: The Royal Society of Chemistry.
25. Vogel S. 2003 *Comparative biomechanics: life's physical world*. Princeton, NJ: Princeton University Press.
26. Alimov MM, Kornev KG. 2014 Singularities of meniscus at the V-shaped edge. *Mech. Res. Commun.* **62**, 162–167. (doi:10.1016/j.mechrescom.2014.10.003)
27. Langbein DW. 2003 *Capillary surfaces: shape–stability–dynamics, in particular under weightlessness*. New York, NY: Springer.
28. Adamson AW, Gast AP. 1997 *Physical chemistry of surfaces*. New York, NY: Wiley.
29. Roy RV, Schwartz LW. 1999 On the stability of liquid ridges. *J. Fluid Mech.* **391**, 293–318. (doi:10.1017/s0022112099005352)
30. Sande LM. 2017 Materials properties of the lepidopteran proboscis and a bio-inspired characterization method of capillary adhesion. Master's thesis, Clemson University, Clemson, SC, USA.
31. Liu YL, Guo H, Huang LQ, Pelosi P, Wang CZ. 2014 Unique function of a chemosensory protein in the proboscis of two *Helicoverpa species*. *J. Exp. Biol.* **217**, 1821–1826. (doi: 10.1242/jeb.102020)
32. Hadley NF. 1994 *Water relations of terrestrial arthropods*. San Diego, CA: Academic Press.
33. Adler PH. 1982 Soil- and puddle-visiting habits of moths. *J. Lepid. Soc.* **36**, 161–173.
34. Knopp MC.N, Krenn HW. 2003 Efficiency of fruit juice feeding in *Morpho peleides* (Nymphalidae, Lepidoptera). *J. Insect Behav.* **16**, 67–77. (doi:10.1023/A:1022849312195)
35. Hikl AL, Krenn HW. 2011 Pollen processing behavior of *Heliconius* butterflies: a derived grooming behavior. *J. Insect. Sci.* **11**, 99. (doi:10.1673/031.011.9901)
36. Burton RL. 1975 Carbohydrate digestion in the adult moth *Heliothis zea*. *J. Insect Physiol.* **21**, 1855–1857. (doi:10.1016/0022-1910(75)90253-X)
37. Eberhard SH, Hrassnigg N, Crailsheim K, Krenn HW. 2007 Evidence of protease in the saliva of the butterfly *Heliconius melpomene* (L.) (Nymphalidae, Lepidoptera). *J. Insect Physiol.* **53**, 126–131. (doi:10.1016/j.jinsphys.2006.11.001)
38. Grant JI, Djani DM, Lehnert MS. 2012 Functionality of a reduced proboscis: fluid uptake by *Phigalia strigataria* (Minot) (Geometridae: Ennominae). *J. Lepid. Soc.* **66**, 211–215. (doi:10.18473/lepi.v66i4.a4)
39. Kristensen NP, Nielsen ES. 1981 Double-tube proboscis configuration in neopseustid moths (Lepidoptera, Neopseustidae). *Int. J. Insect Morphol. Embryol.* **10**, 483–486. (doi:10.1016/0020-7322(81)90027-1)
40. Kornev KG, Salamatin AA, Adler PH, Beard CE. 2017 Structural and physical determinants of the proboscis-sucking pump complex in the evolution of fluid-feeding insects. *Sci. Rep.* **7**, 6582. (doi:10.1038/s41598-017-06391-w)